

Research papers

Phase change material thermal energy storage design of packed bed units



Haobin Liang^a, Jianlei Niu^{a,b,*}, Ratna Kumar Annabattula^c, K.S. Reddy^c, Ali Abbas^{d,e}, Minh Tri Luu^d, Yixiang Gan^{a,e,**}

^a School of Civil Engineering, The University of Sydney, NSW 2006, Sydney, Australia

^b Department of Building Environment and Energy Engineering, The Hong Kong Polytechnic University, Hong Kong

^c Department of Mechanical Engineering, Indian Institute of Technology Madras, Chennai 600036, India

^d School of Chemical and Biomolecular Engineering, The University of Sydney, NSW 2006, Sydney, Australia

^e The University of Sydney Nano Institute (Sydney Nano), The University of Sydney, NSW 2006, Australia

ARTICLE INFO

Keywords:

Phase change material
Thermal energy storage
Packed bed
Performance benchmarking

ABSTRACT

Heat transfer enhancement and optimization are found to be essential for the PCM (phase change material) thermal energy storage design. In this work, the performance advantage of the packed bed PCM storage unit design is analyzed in comparison, and the impacts of key geometric parameters of a packed bed unit were numerically investigated. The optimized shell-and-tube design, based on the hexagonal circle configuration, serves as the benchmark for the comparison. The thresholds of the bed and PCM-capsule diameter ratio, D/d , is found, above which the effective energy storage capacity of the packed bed would be higher than that of an optimal shell-and-tube unit. The threshold of D/d can be quantitatively correlated to the superficial velocity of the heat transfer fluid, providing a pathway for the tailored design of a packed bed PCM thermal storage system. In conclusion, it was found that packed bed units are advantageous due to their larger surface-to-volume ratio, in particular in large-scale applications. This work proposes a numerical analysis based framework to design packed bed PCM storage units in comparison with shell-and-tube units so that a proper type of PCM thermal storage design can be selected under a specific geometric and operational condition.

1. Introduction

Global energy supplies are unstable and are increasingly challenged by growing demands and constraining carbon emissions limits. This has seen a significant increase in the proportion of renewable energy supply in recent years, adding a further challenge to existing energy systems to maintain stable operation [1,2]. By shifting load from on-peak to off-peak hours, energy storage can alleviate the imbalance of the energy supply and demand [3], and can address the intermittent energy supply issues of renewable technologies. Thermal energy storage (TES) can serve small and large scale energy storage requirements, complementing electrical energy storage. Due to their ability to release or absorb large quantities of latent heat, phase change materials (PCMs) are receiving attention these days as important TES materials. Compared with the traditional sensible heat storage approach, latent heat thermal energy storage (LHTES) systems have the potential for higher energy storage capacity and efficiency [3–5].

Despite the high thermal storage density of latent heat storage, the

low thermal conductivity of PCMs around 0.2–0.5 W/(m • K) [6], remains a limiting factor. The LHTES system productivity is highly affected during the phase change process, which could lead to inefficiency in large-scale practical application [7]. Hence, extensive studies have focused on increasing the effective thermal conductivity of PCMs to enhance their heat transfer performance. By combining materials of high thermal conductivity with PCMs and by introducing unit design modifications, the heat transfer inside PCMs could be greatly improved. Previous studies showed that graphene nanoparticles [8], carbon-based fillers [9], metal foams [10] and fins [11] can improve the heat transfer performance by 5–130 times higher.

Two common modalities for the LHTES unit design are the shell-and-tube and the packed bed. Heat transfer enhancement of PCM is found to be essential for the shell-and-tube storage unit design [12]. In comparison, a design framework on the performance evaluation for packed bed PCM storage unit design is lacking. The packed bed TES system is composed of packed solid materials and circulated heat transfer fluid. The solid fillers could be rocks, steel and other materials making use of sensible heat or capsules filled with PCM. By packing a large number of

* Correspondence to: J. Niu, School of Civil Engineering, The University of Sydney, NSW 2006, Sydney, Australia.

** Corresponding author.

E-mail addresses: jian-lei.niu@polyu.edu.hk (J. Niu), yixiang.gan@sydney.edu.au (Y. Gan).

Nomenclature		Subscripts
a_p	particle surface area per unit volume of the packed bed 1/m	<i>sat</i> shell-and-tube
c_p	specific heat capacity kJ/(kg • K)	<i>eff</i> effective
d	capsule diameter m	<i>f</i> fluid
d_i	inner tube diameter m	<i>in</i> inlet
d_o	inner tube diameter m	<i>l</i> liquid
D	tank diameter m	<i>m</i> melting
D/d	diameter ratio -	<i>op</i> optimal
E_{st}	effective energy storage ratio -	<i>out</i> outlet
h	convective heat transfer coefficient W/(m ² • K)	<i>p</i> pump
λ_{int}	interstitial convective heat transfer coefficient W/(m ³ • K)	<i>pb</i> packed bed
h	specific enthalpy kJ/kg	<i>s</i> solid
k	thermal conductivity W/(m • K)	<i>t</i> tube
L	tank height m	<i>w</i> water
L/D	aspect ratio of the tank -	
H	latent heat kJ/kg	
Q_{eff}	effective energy storage capacity J	
Q_∞	theoretical energy storage capacity J	
q_c	charging rate W	
t	time s	
T	temperature K	
u	interstitial fluid velocity m/s $u = (4\dot{V}) / (\varepsilon\pi D^2)$	
u_{sup}	superficial fluid velocity m/s $u_{sup} = (4\dot{V}) / (\pi D^2)$	
V	volume m ³	
\dot{V}	volumetric flow rate m ³ /s	
\mathbf{v}	velocity vector m/s	
		Greek letters
		ε void fraction -
		λ PCM volume ratio -
		φ capacity effectiveness -
		η heat transfer effectiveness -
		ρ density kg/m ³
		μ dynamic viscosity Pa • s
		Abbreviations
		HTF heat transfer fluid
		LHTES latent heat thermal energy storage
		PCM phase change material
		TES thermal energy storage

PCM sphere capsules, the surface-to-volume ratio is increased, resulting in a higher heat transfer rate [13]. Besides, encapsulation shows advantages in preventing chemical reactions, improving material compatibility and making the phase change process more flexible [14]. The effects of the inlet temperature and flow rate of heat transfer fluid have been widely investigated and it was generally concluded that with the increase of the difference between inlet temperature and phase change temperature and the increase of inlet flow rate, the charging or discharging rate would be higher [15–17]. Besides, a smaller capsule diameter is beneficial to increase the effective discharging efficiency [16] and the charging rate [17]. The heat transfer in a packed bed LHTES unit could be further improved by enhancing the effective thermal conductivity of PCM capsules. By encapsulating PCM with expanded graphite, the effective thermal conductivity can be increased by 12 times, from 0.6 to 7.2 W/(m • K) [18]. Besides, by inserting aluminium alloy [19] and fins [20] into the spherical capsule, the phase change time could be greatly shortened by up to 50%. Recent studies on packed bed PCM storage found that the radial porosity oscillation of PCM capsules would lead to non-uniform velocity distribution of fluid [21]. Kumar and Saha [22] explored the potential of cylindrical PCM capsules as an alternative to develop a leakproof and low-cost solution and pointed out the importance of considering the thermal stress in the tank wall in the design. Grabo et al. [23] found that super-ellipsoidal PCM capsules with holes and grooves can achieve higher packing densities and enhance heat transfer, contributing to a 20% increase in energy density. Moreover, multi-layered packed bed TES systems, with varying PCM melting temperature along the flow direction, has been research interests in recent years, as they can improve the stratification in the storage tank and thus leads to higher charging rates, energy/exergy efficiencies [24–26].

Several numerical approaches are mainly adopted by current numerical studies on packed bed TES system performance, including the single phase model [27], Schumann's model [17], concentric dispersion model [28,29] and continuous solid phase model [30,31]. The single

phase model considers heat transfer fluid (HTF) and PCM as one phase and thus can be only applicable when the solid has both high thermal conductivity and thermal capacity compared with HTF [32]. In comparison, by considering the capsule and HTF as two separate phases, the concentric dispersion model shows advantages in solving the thermal gradient inside PCM and the continuous solid phase model is capable of solving thermal conduction in the radial and axial directions [33]. In contrast, Schumann's model considers neither heat conduction nor thermal diffusion inside solid capsules [34].

Even though packed bed TES units show higher charging and discharging rates, compared with storage units with bulk PCMs [29], more than 70% of LHTES studies focus on the shell-and-tube type [35]. The influences of design parameters on a shell-and-tube TES unit have been widely studied [36,37] and the charging/discharging time and phase change fraction are the main indicators to measure energy storage performance. With benchmarking to the traditional shell-and-tube units, we aim to develop a design framework on the performance evaluation for packed bed PCM storage unit design. As a result, this paper presents a model-based design framework for the packed bed TES unit, by maximizing the effective energy storage ratio E_{st} [37]. The impacts of geometric parameters (capsule diameter d , tank diameter D and tank height L) and effective thermal conductivity k_{eff} are investigated. The packed bed TES unit's E_{st} is compared with one of the optimal shell-and-tube units under the same tank aspect ratio and HTF superficial velocity. The optimal shell-and-tube design, based on the hexagonal circle configuration, serves as the benchmark for the comparison. The thresholds of the bed and PCM-capsule diameter ratio D/d are found, above which E_{st} of the packed bed would be higher than that of an optimal shell-and-tube design. A comparison of the two scenarios against the packed bed unit is analyzed under different design parameters (aspect ratio of the tank L/D) and operational parameters (superficial velocities u_{sup}). The thresholds of diameter ratio D/d provide a pathway for the tailored design of a packed bed PCM storage.

In this work, the concentrated solar power (CSP) plant, a promising

solution for heating and power generation [24,38], is selected as the energy application for the analysis of packed bed PCM units. The application is used as an example to illustrate the concept of “thresholds of bed and PCM-capsule diameter ratio” to assist design and the methodology can be potentially generalized for the packed bed units under other scenarios. The advantage of packed bed PCM units under higher flow rates by maintaining a large surface-to-volume ratio is exhibited. The numerical analysis based framework proposed could serve as a guideline for designing packed bed LHTES systems, and the study's model-based method can be a reference for designers in their choice of the design modality, based on specific geometric and operational parameters.

2. Methodology

2.1. System configuration

As two mostly implemented types of TES systems using PCM, the schematic of the packed bed and shell-and-tube systems are shown in Fig. 1. In the packed bed system, PCM is encapsulated in capsules with HTF flowing through the spheres. In contrast in the shell-and-tube system, HTF flows through the inner tubes and PCM exists in the bulk form between the inner tube wall and the tank wall.

Based on the geometry of packed bed and shell-and-tube, the key performance index, effective energy storage ratio E_{st} [37] for the thermal storage system is defined in Eqs. (1)–(3). The effective energy storage capacity Q_{eff} indicates the actual amount of the heat stored when charging, while Q_{HTF} is the ultimate energy storage capacity of an ideal stratified sensible heat storage system with the heat transfer fluid used for the LHTES system, which is Therminol Vp1 in this study. Therefore, Q_{HTF} serves as a benchmark for the TES system using PCM and an LHTES system with E_{st} larger than one means that the latent heat storage outperforms the stratified sensible heat storage. T_0 and V refer to the initial temperature and volume of the sensible or latent heat storage system, respectively. For the packed bed, since the 1D continuous phase model is

used in this study, T_{out} is directly the outlet temperature calculated by simulation. As for the shell-and-tube, T_{out} is calculated as the mass-weighted average temperature at the tube outlet, as shown in Eq. (4).

$$E_{st} = \frac{Q_{eff}}{Q_{HTF}} \quad (1)$$

$$Q_{HTF} = \rho_f c_{p,f} V (T_{in} - T_0) \quad (2)$$

$$Q_{eff} = \int_0^{t_{eff}} \dot{m} c_{p,f} (T_{in} - T_{out}) dt \quad (3)$$

$$T_{out} = \frac{\int_0^{d_i} T(r) \bullet \rho_f u(r) \bullet 2\pi r dr}{\dot{m}} = \frac{\int_0^{d_i} T(r) u(r) r dr}{\int_0^{d_i} u(r) r dr}. \quad (4)$$

The effectiveness-NTU theory [39,40] has been applied to determine the effective energy stored and to measure the performance of LHTES units in this study. As a concept originally developed for heat exchangers, the effectiveness is the ratio of the actual heat transfer rate to the maximum possible heat transfer rate [41]. For an LHTES unit, the heat transfer effectiveness is characterized as the temperature difference between inlet and outlet over the maximum temperature difference, shown in Eq. (5) [39]. NTU (number of heat transfer units) is defined as $(UA)/(m c_p)$, where U is overall heat transfer coefficient, A is heat transfer area, \dot{m} is fluid mass flow rate and c_p is fluid specific heat capacity. For the charging process, the PCM temperature used to measure the maximum temperature difference is the melting temperature. The sensible energy of the PCM has been ignored in the definition of η , as the effect is negligible considering the amount of latent heat [39].

$$\eta = \frac{T_{in} - T_{out}}{T_{in} - T_m} = 1 - e^{-NTU} \quad (5)$$

According to Eq. (5), during the charging process, the heat transfer effectiveness η drops, when the outlet temperature rises. A minimum η should be determined, to make sure that the heat transfer between HTF

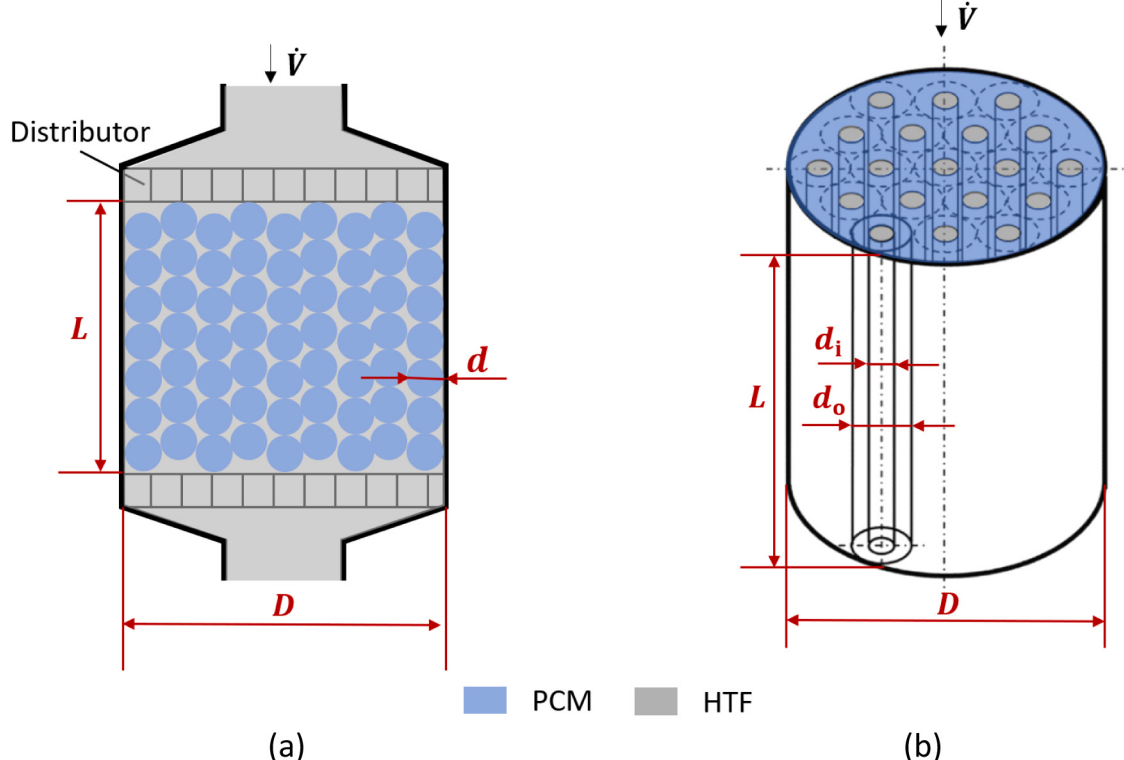


Fig. 1. Schematic of LHTES design modalities: (a) Packed bed; (b) Shell-and-tube.

and PCM is still effective. $\eta = 0.8$ was chosen as the minimum value in this study. Thus, the outlet temperature should not exceed a certain value, which is called the cut-off temperature, to ensure the effectiveness is larger than 0.8. The energy stored before reaching the minimum heat transfer effectiveness is calculated as the effective energy storage capacity Q_{eff} , shown in Eq. (3). As illustrated above, controlling the outlet temperature of the heat transfer fluid ensures the heat transfer effectiveness between PCM and HTF in the storage system. In addition, there may exist direct requirements on the outlet temperature in applications. For example, when discharging the heat released by devices in data centers and storing it in the TES system, the outlet temperature of HTF must be controlled under a certain value before it is circulated back to device cooling, to avoid damage to devices due to high temperature.

The theoretical energy storage capacity Q_{∞} , the capacity effectiveness φ and the theoretical effective energy storage ratio $E_{\text{st}, \infty}$ are defined in Eqs. (6)–(9), to indicate the energy has been stored compared with the maximum value in a storage unit with PCM. V is the storage unit volume and ε is the void fraction, which is the percentage of HTF in the LHTES unit. The charging rate q_c measures the energy storage efficiency regarding time.

$$Q_{\infty} = (1 - \varepsilon)\rho_{\text{PCM}} V [c_{\text{p,PCM}}(T_{\text{in}} - T_0) + H] + \varepsilon\rho_f c_{\text{p,f}} V(T_{\text{in}} - T_0) \quad (6)$$

$$\varphi = \frac{Q_{\text{eff}}}{Q_{\infty}} \quad (7)$$

$$E_{\text{st}, \infty} = \frac{Q_{\text{eff}}}{Q_{\text{HTF}}} \quad (8)$$

$$q_c = \frac{Q_{\text{eff}}}{t_{\text{eff}}} \quad (9)$$

An illustration of the above-mentioned indices including E_{st} , Q_{eff} , Q_{∞} , Q_{HTF} and q_c are represented in Fig. 2. In this study, the performance of the packed bed and shell-and-tube storage unit is mainly estimated by the effective energy storage ratio E_{st} . In general, a value of E_{st} indicates effective thermal storage with PCM as the storage unit outperforms the one utilizing sensible heat. A larger value of E_{st} is more desirable as the effective energy storage capacity is higher. The goal when designing a TES unit with PCM is to maximize the key performance index E_{st} and the index could be used to compare the storage performance of packed bed and shell-and-tube storage units.

2.2. Comparison approach

A single concentric cylinder unit was simulated for the shell-and-tube unit, with a hypothetical outer tube to approximate the hexagon boundary between the tubes, as shown in Fig. 3. Therefore, the cross-

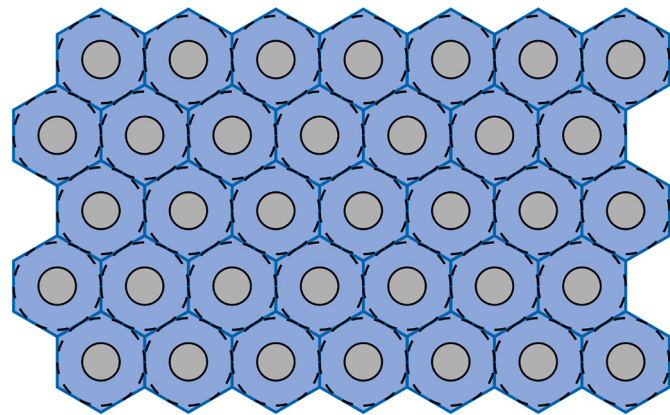


Fig. 3. Hexagonal circle packing assumption

sectional area ratio of the inner tube and hexagon boundary in the shell-and-tube tank can be compared to the void fraction ε for a packed bed, and calculated as follows:

$$\varepsilon_{\text{tank}} = \frac{\sqrt{3}\pi}{6} \frac{d_i^2}{d_o^2} \quad (10)$$

The inner tube diameter d_i was chosen as 10 mm for the concentric cylinder unit. For the packed bed system, when the diameter ratio D/d is varying between 4 and 21, the void fraction ε varies from 0.40 to 0.44. As for the shell-and-tube unit, an optimal PCM volume ratio λ_{op} exists by varying the outer tube diameter [36]. The PCM volume ratio λ is calculated as $1 - d_i^2/d_o^2$, which means that the void fraction of a shell-and-tube tank could be more variable than that of a packed-bed.

The circle packing number n_t , i.e. the number of inner tubes, could be obtained as the area ratio of tank's cross-section over hexagon, shown in Eq. (11):

$$n_t = \frac{\frac{\pi D^2}{4}}{\frac{6d_o^2}{4\sqrt{3}}} = \frac{\sqrt{3}\pi}{6} \frac{D^2}{d_o^2}. \quad (11)$$

Therefore, the inlet velocity and Reynolds number of the inner tube of the concentric cylinder unit could be calculated after the volumetric flow rate is specified:

$$u_{\text{in}} = \frac{4\dot{V}}{n_t \cdot \pi d_i^2}, \quad (12)$$

$$Re_t = \frac{\rho_f d_i u_{\text{in}}}{\mu_f} = \frac{4\rho_f \dot{V}}{n_t \mu_f \pi d_i}. \quad (13)$$

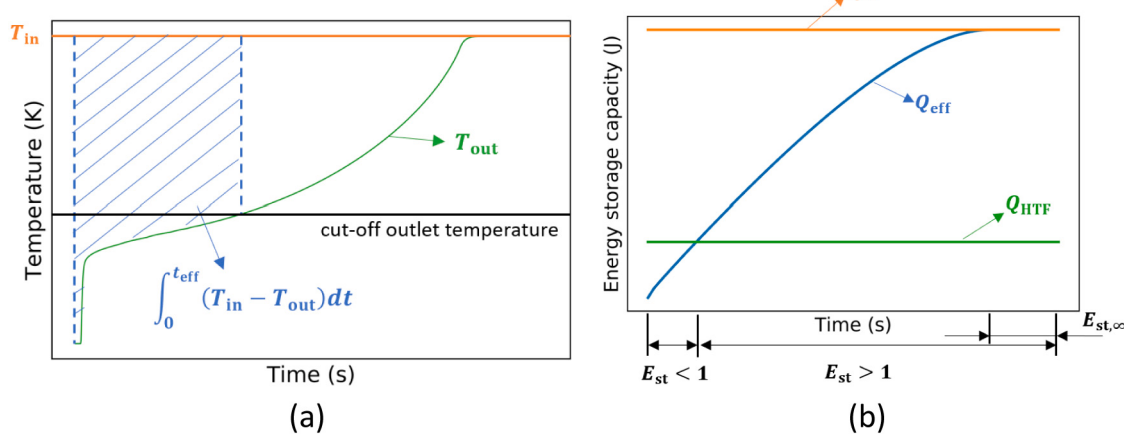


Fig. 2. Illustration of indices used in this study: (a) Calculation of effective energy storage ratio Q_{eff} ; (b) Relationship among E_{st} , $E_{\text{st}, \infty}$, Q_{eff} , Q_{∞} , Q_{HTF} .

For the comparison purpose, the tank diameter D was set as 250 mm for both shell-and-tube and packed bed tanks. The tank length L and superficial velocity $u_{\text{sup}} = (4V)/(\pi D^2)$, which varies in parametric studies, were kept the same when comparing. The superficial velocity is defined as the flow velocity given the cross-sectional area of the tank. It should be noted that when the volumetric flow rate is changing, the Reynolds number is also changing according to Eq. (13).

2.3. Numerical model

The commercial modeling software COMSOL Multiphysics 5.3a (COMSOL, Inc., USA), was used for the numerical simulation. For the simulation of the packed bed, as temperature variations over time and tank height for HTF are the main concerns to study the effective energy storage capacity in this paper, 1D continuous solid phase model was applied to study the heat transfer of both HTF and PCM in the packed bed TES system. The model shows reasonable consistency with experimental results, which is shown in the validation part.

2.3.1. Governing equations

For packed bed systems, the energy equations [30] of HTF and PCM are as follows, which takes the local thermal non-equilibrium as the assumption:

$$\varepsilon c_{p,f} \rho_f \left(\frac{\partial T_f}{\partial t} + u \frac{\partial T_f}{\partial y} \right) = k_f \frac{\partial^2 T_f}{\partial y^2} + \kappa_{\text{inter}} (T_{\text{PCM}} - T_f) \quad (14)$$

$$(1 - \varepsilon) c_{p,\text{eff}} \rho_{\text{PCM}} \frac{\partial T_{\text{PCM}}}{\partial t} = k_{\text{eff}} \frac{\partial^2 T_{\text{PCM}}}{\partial y^2} + \kappa_{\text{inter}} (T_f - T_{\text{PCM}}) \quad (15)$$

The interstitial fluid velocity can be derived through the volumetric flow rate: $u = 4V/(\varepsilon \pi D^2)$. When the conduction resistance in the solid cannot be neglected, an effective heat transfer coefficient h_{eff} can be estimated by Eq. (16) [42], in which coefficient n depends on the solid shape and for sphere $n = 10$. The effective heat transfer coefficient method gives good results and has been applied by previous studies in packed bed system simulations [43,44].

$$\frac{1}{h_{\text{eff}}} = \frac{1}{h} + \frac{d}{k_{\text{PCM}} \bullet n} \quad (16)$$

$$\kappa_{\text{inter}} = h_{\text{eff}} a_p \quad (17)$$

$$a_p = \frac{6(1 - \varepsilon)}{d} \quad (18)$$

In Eqs. (16)–(17), κ_{inter} is the interstitial convective heat transfer coefficient and a_p is the particle surface area per unit volume of the packed bed. It should be pointed out that the bulk PCM thermal conductivity k_{PCM} used in Eq. (16) was adopted as the effective thermal conductivity of the solid in a packed bed k_{eff} , which ignores the influence of contact conduction on the effective thermal conductivity. This is acceptable as conduction is a second-order phenomenon compared to convective heat transfers and the characteristic time of conduction is much lower than convection one [42]. Therefore, for simplification, the analysis of the effective thermal conductivity's influences on the packed bed storage capacity in Section 3.2 refers to the thermal conductivity of bulk PCM. The empirical Nusselt number correlation [45] for the fluid-solid interface could be used to calculate the convective heat transfer coefficient h . The calculation of dimensionless number and void fraction [46] are given in Eqs. (19)–(21).

$$\text{Nu} = 2 + 1.1 \text{Re}^{0.6} \text{Pr}^{\frac{1}{3}} = \frac{hd}{k_f} \quad (19)$$

$$\text{Re} = \frac{\rho_f (\varepsilon u) d}{\mu_f}, \text{Pr} = \frac{\mu_f c_{p,f}}{k_f} \quad (20)$$

$$\varepsilon = 0.4 + 0.05 \left(\frac{d}{D} \right) + 0.412 \left(\frac{d}{D} \right)^2, \frac{d}{D} \leq 0.5 \quad (21)$$

To effectively describe packed beds using the above continuum equations requires a minimum mesh size to be sufficiently larger than the feature size, i.e., particle size d . For the numerical model, the sampled volume should be large enough to represent its entity, satisfying the continuum assumption that local fluctuations can be volumetrically averaged. In this study, as the axial element with a mesh size of dy in the one-dimensional model is an average value of the radial cross-section of a 3D volume of $\pi D^2 dy / 4$, the packed bed would satisfy the continuum assumption if this representative volume is sufficiently larger than the unit cell volume of $\pi d^3 / 6(1 - \varepsilon)$. Dixon [47] suggested that for packed bed containing spheres, the pseudo-continuum models are reasonable down to the tube-to-diameter ratio equal to 4. Thus, D/d is controlled to be larger than 4 in this study, to ensure the validity of the continuous solid phase model.

As shown in Fig. 3 (a), the 2D axisymmetric domain representing a concentric cylinder in the shell-and-tube system was simulated. Eqs. (22)–(24) indicate the continuity, momentum and energy equations for heat transfer fluid. As for the PCM domain, the heat transfer equation is shown in Eq. (25). Conjugate heat transfer was applied through the Non-Isothermal Flow module in COMSOL. The inlet temperature and velocity of the heat transfer fluid, and the pressure at the outlet were determined as the boundary conditions. For the fluid flow module, no-slip condition was applied to the wall of the inner tube. As for the heat transfer module, thermal resistance between fluid and PCM has been neglected and all boundaries except the inlet and outlet were assumed as thermally insulated.

$$\rho_f \nabla \bullet (\mathbf{v}) = 0 \quad (22)$$

$$\frac{\partial \mathbf{v}}{\partial t} + \rho_f (\mathbf{v} \bullet \nabla) \mathbf{v} = \nabla \bullet [-p + \mu_f (\nabla \mathbf{v} + (\nabla \mathbf{v})^T)] + \rho_f g \quad (23)$$

$$\rho_f c_p \frac{\partial T_f}{\partial t} + \rho_f c_{p,f} \mathbf{v} \bullet \nabla T_f + \nabla \bullet (-k_f \nabla T_f) = 0 \quad (24)$$

$$\rho_{\text{PCM}} c_{p,\text{eff}} \frac{\partial T_{\text{PCM}}}{\partial t} + \nabla \bullet (-k_{\text{PCM}} \nabla T_{\text{PCM}}) = 0 \quad (25)$$

2.3.2. Effective heat capacity model

The effective heat capacity method is applied to solving the PCM domain for both packed bed and shell-and-tube units. By considering the phase change range of PCM, more precise results could be obtained. The method assumes PCM's specific heat as a function of temperature $c_{p,\text{eff}} = f(T)$, which takes the latent heat during the phase change process into account.

As shown in Fig. 4, the enthalpy for PCM is defined with a modified

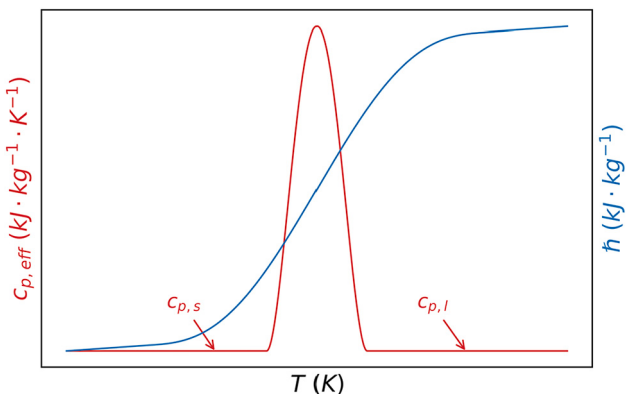


Fig. 4. The effective specific heat method: effective specific heat capacity $c_{p,\text{eff}}$ and specific enthalpy h

step function $\sigma(x)$, which has the transition zone size as PCM phase change temperature range. In Eq. (26), T_m refers to the melting temperature of PCM and H indicates the latent heat. The first term on the right side represents the enthalpy contributed by the sensible heat of PCM. The melting temperature is determined by the start and end temperature, T_s and T_l , of the melting process, shown in Eq. (27). Hence, the effective specific heat capacity $c_{p,\text{eff}}$ in the heat transfer governing equation is a piecewise function shown in Eq. (28), in which the effective heat capacity during the phase change is represented by the derivative of the enthalpy function over temperature.

$$\dot{h} = c_{p,s}T + H \bullet \sigma(T - T_m) \quad (26)$$

$$T_m = \frac{T_s + T_l}{2} \quad (27)$$

$$c_{p,\text{eff}} = \begin{cases} c_{p,s}, & T \leq T_s \\ \frac{dh}{dT}, & T_s < T < T_l \\ c_{p,l}, & T \geq T_l \end{cases} \quad (28)$$

The direct solver of PARDISO and MUMPS was applied for shell-and-tube and packed bed respectively during the simulation. As for the time-dependent solver, segregated method and fully coupled method were applied for shell-and-tube and packed bed, respectively. The absolute tolerance for solvers was 0.0001. The spatial and temporal discretization schemes are shown in Section 2.5.

2.4. Model validation

The results of the PCM charging process from the experimental study of Nallusamy et al. [15] were adopted to validate the numerical model of the packed bed system. The parameters for the packed bed TES system and PCM properties used in the experiment are specified in Table 1.

The HTF temperatures at the middle height and the outlet of the tank ($y/L = 0.5, y/L = 1$) were chosen for the validation. The independence of the mesh and time step was checked during the validation process. The mesh size of 10 mm and the time step of 1 s were adopted for validation. As shown in Fig. 5, there exists a discrepancy in PCM temperature between experimental and numerical results. This could be explained by the fact that in the numerical model, PCM is considered as a continuous phase. However, in experiments temperature at a single point is measured inside a capsule and the thermal gradients exist inside a single capsule. Note that the bulk thermal conductivity of PCM is relatively low, thus providing noticeable temperature difference, even within

Table 1
System parameters and PCM properties [15] for validation.

System Parameter	Value
Tank height (m)	0.46
Tank diameter (m)	0.36
Spherical capsule diameter (mm)	55
Flow rate (L/min)	2
Inlet temperature (°C)	70
Initial temperature (°C)	32
Void fraction (-)	0.5

PCM Property	Value
Latent heat capacity (kJ/kg)	213
Melting temperature (°C)	60 ± 1
Specific heat capacity (solid) (kJ/(kg • K))	1.85
Specific heat capacity (liquid) (kJ/(kg • K))	2.384
Thermal conductivity (solid) (W/(m • K))	0.4
Thermal conductivity (liquid) (W/(m • K))	0.15
Density (solid) (kg/m ³)	861
Density (liquid) (kg/m ³)	778

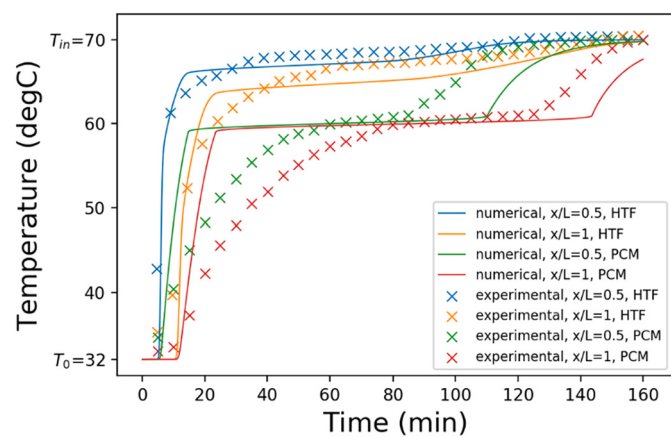


Fig. 5. Validation of packed bed unit against experimental data [15]

single capsules. On the other hand, HTF temperature varying with time from numerical simulations fits well with the experimental results and thus the error is considered within the acceptable range. Since in this study, HTF temperature is the main concern to estimate the effective energy storage ratio E_{st} , the validation results show that the numerical model is reliable enough to analyze the overall storage performance of the packed bed storage unit.

As for the concentric cylinder unit in shell-and-tube systems, the validation results and corresponding parameters for validation can be found in the previous publication [36].

2.5. Parametric studies for design comparison

The default settings for the design comparison of packed bed and shell-and-tube are specified in this section. For the heat transfer fluid domain, the initial temperature T_0 , inlet temperature T_{in} and superficial velocity u_{sup} are 192 °C, 252 °C and 0.00340 m/s, respectively. The initial temperature of PCM is the same as the one of HTF, i.e. 192 °C. The properties of PCM [48] and HTF are shown in Table 2, in which HTF properties are specified as the ones when the temperature is 220 °C [49]. As indicated in Section 2.1, the minimum heat transfer effectiveness is $\eta = 0.8$ and the according cut-off outlet temperature is 228 °C. When the outlet temperature reaches the outlet temperature, the charging process stops and the effective energy storage capacity is calculated.

The base geometric parameters for the packed bed were set as $L = 2$ m, $D = 0.25$ m, $d = 30$ mm. The mesh sensitivity was analyzed and eventually the mesh size of 10 mm and the time step of 0.1 s was chosen for studying the geometric parameters of the packed bed. As for the system comparison study, the superficial velocity, tank height and tank diameter were kept the same for both systems.

Table 2
PCM and HTF properties used in this study.

PCM: Solar Salt (60% NaNO ₃ + 40%KNO ₃)	HTF: Therminol Vp1 (Biphenyl/diphenyl oxide mixture)		
H (kJ/kg)	161	μ (Pa • s)	0.000345
T_m (°C)	222	ρ (kg/m ³)	895
ΔT (°C)	40	c_p (J/(kg • K))	2101
ρ (kg/m ³)	1924	λ (W/(m • K))	0.1106
c_p (J/(kg • K))	1490		
λ (W/(m • K))	0.5		

3. Results and discussions

3.1. The effect of geometric parameters on the packed bed

Based upon the default parameter settings ($L = 2$ m, $D = 0.25$ m, $d = 30$ mm, $\dot{V} = 10$ liter/min) and specified mesh size and time step, the numerical simulation for a two-hour PCM charging process was completed. The temperature distributions of HTF and PCM in the packed bed TES system are shown in Fig. 6. The figure shows the temperature every four minutes in the axial direction. It could be seen that as time increases, the temperature of both PCM and HTF increases. Meanwhile, the temperature increase rate of PCM is lower than that of HTF. After two hours of charging, PCM and HTF temperature in the whole tank reaches the inlet temperature, which means that there exists no more heat transfer and effective energy storage from HTF to PCM, according to Eq. (3).

To investigate the dimensionless geometric effects on the effective energy storage performance in the packed bed LHTES system, a group of parametric studies were performed. The diameter ratio in this study satisfies $D/d > 5$ and different combinations of D , d and L are sampled for parametric studies. To obtain 8 sets of diameter ratios D/d including 5.56, 7.71, 9.33, 11.60, 13.18, 15.00, 17.65 and 20.67, descending capsule diameter d and ascending tank diameter D are combined. The combinations of (d, D) in the unit of (mm, m) are specified as follows: (45, 0.25), (35, 0.27), (30, 0.28), (25, 0.29), (22, 0.29), (20, 0.30), (17, 0.30) and (15, 0.31). The tank height L of 1 m, 2 m, 3 m, 5 m, 7 m and 9 m are adopted to be combined with the above-mentioned eight diameter ratio D/d values to obtain 48 sets of studies. Another 15 sets of parametric studies for higher L/d are added by increasing L . The additional combinations of $(D/d, L)$ are as follows: (5.56, 15 m), (5.56, 20 m), (5.56, 25 m), (7.71, 12 m), (7.71, 15 m), (7.71, 19 m), (9.33, 13 m), (9.33, 17 m), (11.60, 11 m), (11.60, 14 m), (13.18, 10 m), (13.18, 12 m), (15.00, 10 m), (15.00, 11 m), (17.65, 10 m). Under the superficial velocity of 0.00340 m/s, the results of the total 63 sets of parametric studies are shown in Fig. 7.

Fig. 7 exhibits how the effective energy storage ratio E_{st} varies as the two dimensionless geometric parameters D/d and L/d . It can be observed that as either D/d or L/d increases, the energy storage performance is enhanced. One thing that should be noted in this figure is that only when both D/d and L/d are small (eg. $D/d = 5.56$, $L/d = 22.2$), the packed bed LHTES system is ineffective ($E_{st} = 0.794 < 1$). However, the storage systems are effective for all other cases ($E_{st} > 1$). In other words, as long as the diameter ratio D/d is larger than 8 or the length ratio L/d is larger than 45, the system can be ensured to be effective. In addition, no significant enhancement E_{st} is shown when D/d is larger than around 12 and when L/d is approximately higher than 100. As shown in the figure, the 3D plot is nearly a plateau as D/d and L/d gets larger. This is because E_{st} is approaching the theoretical effective energy

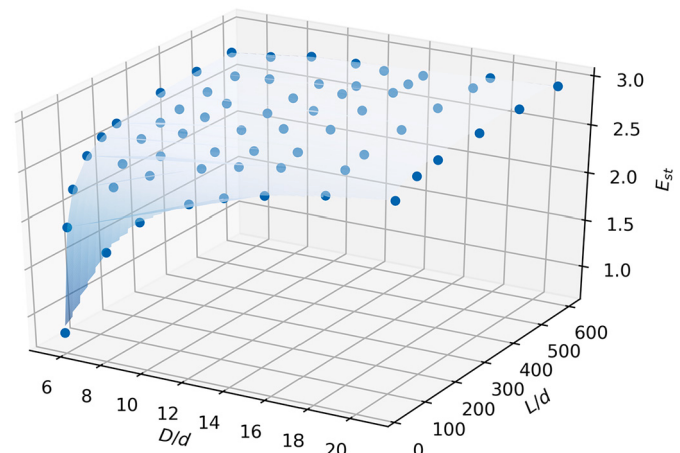


Fig. 7. Dimensionless scaling: E_{st} vs D/d and L/d

storage ratio $E_{st,\infty}$, which is the maximal energy that could be stored in the LHTES system under given parameters.

It should be mentioned that even though E_{st} increases as d decreases, the pressure drop over the entire tank increases in the meantime. Therefore, it is necessary to estimate the variation of energy consumption while changing the capsule size. The Ergun equation shown in Eq. (29) is applied in the study to estimate the pressure drop over the packed bed system and Eq. (30) estimates the energy consumed by the pump due to the pressure drop.

$$\frac{\Delta p}{L} = 150 \frac{(1-\varepsilon)^2}{\varepsilon^3} \frac{\mu_f u}{d^2} + 1.75 \frac{(1-\varepsilon)}{\varepsilon^3} \frac{\rho_f u^2}{d} \quad (29)$$

$$Q_{\text{pump}} = \Delta p \dot{V} t \quad (30)$$

It was found that a smaller capsule diameter leads to a higher percentage of energy consumption over energy storage $Q_{\text{pump}}/Q_{\text{eff}}$. However, even when d is 10 mm, $Q_{\text{pump}}/Q_{\text{eff}}$ is still smaller than 1e-4%, which means that the effect of an increase in energy consumption on the packed bed TES system could be neglected, under the specified conditions. It should be noted that a smaller capsule size would result in more capsules required for packing, and thus the investment cost of the packed bed unit could increase significantly.

In conclusion, the dimensionless scaling analysis provides the designer with a more objective approach to choosing design parameters, by maximizing the effective energy storage ratio. As for a specific application, the energy storage ratio over costs could be calculated to estimate the economic aspects of the packed bed LHTES system.

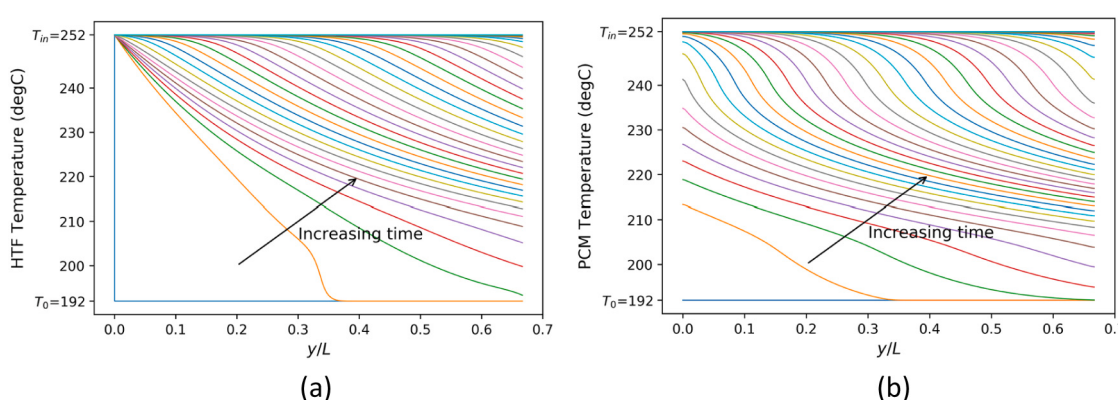


Fig. 6. Temperature distribution in the packed bed TES system of the two-hour charging process: (a) HTF; (b) PCM

3.2. The effect of the effective thermal conductivity k_{eff}

By encapsulating PCM with expanded graphite or inserting metal fins into PCM capsules, a higher effective thermal conductivity of PCM and a higher phase change rate could be achieved. This section examines the influences of the effective thermal conductivity k_{eff} on the energy storage performance of the packed bed unit. As specified in Section 2.3.1, to simplify the analysis, the PCM thermal conductivity was regarded as k_{eff} in the numerical model. The tank height, tank diameter and superficial velocity were fixed at 5 m, 0.25 m and 0.0170 m/s, respectively. The effective thermal conductivities were selected as 0.5, 1, 2, 5 W/(m · K). The capsule diameters d were chosen as 10, 12.5, 20, 30, 40, 50 and 60 mm. Consequently, the diameter ratios D/d vary between 4.2 and 25.

The heat transfer in packed bed is composed of three parts: conduction in heat transfer fluid, interface convection between fluid and PCM and conduction in PCM [42,50]. It should be noted that the natural convection occurring in liquid PCM can be reflected by the effective thermal conductivity [38]. As shown in Fig. 8, the increase of k_{eff} leads to increasing E_{st} , indicating a more effective storage unit. This is because a higher k_{eff} results in a lower PCM thermal resistance and thus the total heat transfer is enhanced. However, it could be observed that the influence of effective energy storage enhancement is less significant when the diameter ratio is large, especially when D/d is 20 and 25. Both large D/d and large k_{eff} contribute to the heat transfer enhancement in a packed bed unit, through enhancing convection and reducing PCM thermal resistance, which is reflected in higher E_{st} . Therefore, when D/d is higher, the contribution to enhanced heat transfer by increasing k_{eff} is less influential. Hence, mixing PCM with high thermal conductivity materials is recommended when D/d is limited at a lower level for a packed bed LHTES unit. In this study, the enhancement effect is significant when D/d is smaller than 12.5.

3.3. Design comparison

As specified in Section 2.2, the comparison of energy storage performance between shell-and-tube and packed bed units was completed by assuming the 2D hexagonal circle packing for the shell-and-tube cylinder unit in a tank. Moreover, the tank diameter D (0.25 m), tank height L (0.25, 1, 3, 5, 7, 9 m) and superficial velocity u_{sup} (0.00340, 0.0170, 0.0306 m/s) were kept the same for both units. Thus, the aspect ratios of the tank L/D for both shell-and-tube and packed bed units are 1, 4, 12, 20, 28 and 36. As the void fraction of a shell-and-tube tank could be more variable than that of a packed bed, the performance of packed bed storage unit is compared with two scenarios of the shell-and-tube unit:

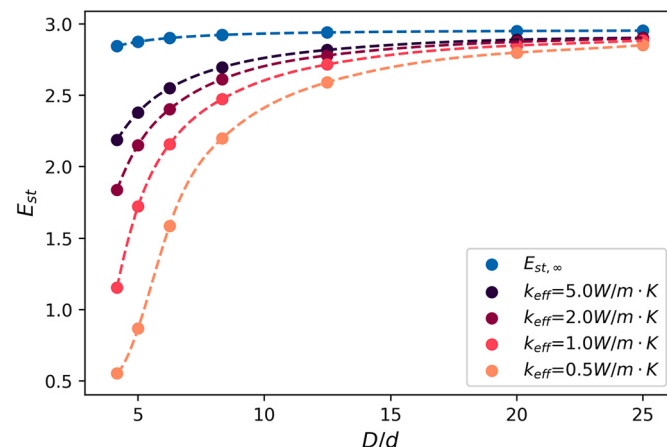


Fig. 8. The impacts of effective thermal conductivity k_{eff} on the effective energy storage ratio E_{st} of packed bed storage unit

- Optimal PCM volume ratio under the thermal conductivity of pure PCM, i.e. 0.5 W/(m · K);
- Optimal PCM volume ratio with enhanced effective thermal conductivity of 5 W/(m · K).

The inner tube diameter of the shell-and-tube cylinder unit d_i was assumed as 10 mm and the PCM volume ratio λ for the simulated unit is $1 - d_i^2/d_o^2$. While changing the PCM volume ratio for the shell-and-tube concentric unit, the Reynolds number of the internal HTF varied between 118 and 1479, which means that the flow is laminar. As the fully turbulent flow generally exhibits a lower maximal effective energy storage ratio $E_{\text{st}, \text{op}}$ than laminar flow [36], and therefore only laminar flow scenarios have been discussed in this study. As for the packed bed, the capsule diameters d were chosen as 10, 12.5, 15, 20, 30, 40, 50 mm and consequently the diameter ratios D/d varied between 5 and 25. The design parameters for comparison are summarized in Table 3. In the section, the results compare the effective energy storage ratio E_{st} , charging rate q_c and capacity effectiveness φ for shell-and-tube and packed bed TES units using PCM under different superficial velocities and aspect ratios of the tank.

Fig. 9 exhibits an example of the effective energy storage ratio comparison when the superficial velocity is 0.00340 m/s and the aspect ratio of the tank L/D for both shell-and-tube and packed bed unit is 12. The effective thermal conductivity was kept as 0.5 W/(m · K) for the packed bed unit. As shown in Fig. 9 (b), the optimal PCM volume ratio for shell-and-tube is found by varying the outer tube diameter. It should be pointed out that while increasing the PCM volume ratio for simulation, the packing number of tubes decreases and the inlet velocity of HTF consequently increases. Therefore, the effective energy storage ratio remains lower compared with the fixed inlet velocity scenario. In Fig. 9 (a), circle scatter points represent the effective energy storage ratio of the packed bed under different diameter ratios D/d and the blue dashed line is obtained after interpolation. The optimal effective energy storage ratios of the shell-and-tube unit when the effective thermal conductivity is 0.5 and 5 W/(m · K) are marked with the cross points. The threshold of D/d for the packed bed unit is thus obtained.

The threshold of D/d is an indicator for choosing a proper type of storage unit, which is obtained by considering the same energy storage performance between shell-and-tube and packed bed. Specifically, when designing the packed bed LHTES unit, if the diameter ratio D/d is smaller than the threshold, it means energy storage of the shell-and-tube unit is more effective and should be chosen. On the other hand, if D/d is larger than the threshold, then the packed bed unit outperforms the shell-and-tube unit under the specified scenario and is preferable. The value of the threshold informs the designer whether the packed bed unit should be chosen over the shell-and-tube unit. A higher threshold of D/d indicates that it is more difficult for the packed bed to achieve the same energy storage performance as the shell-and-tube unit. In this case, the shell-and-tube unit would be more advantageous. The comparison plots as shown in Fig. 9 (a) under other superficial velocities and tank aspect ratios could be found in Appendix B.

Table 3
Design parameters for comparison

Storage unit	Shell-and-tube	Packed bed
Tank diameter D (m)	0.25	0.25
Tank height L (m)	0.25, 1, 3, 5, 7, 9	0.25, 1, 3, 5, 7, 9
Aspect ratio of tank L/D (-)	1, 4, 12, 20, 28, 36	1, 4, 12, 20, 28, 36
Superficial velocity u_{sup} (m/s)	0.00340, 0.0170, 0.0306	0.00340, 0.0170, 0.0306
Diameter ratio D/d (-)	-	5, 6.25, 8.3, 12.5, 16.7, 20, 25
Inner tube diameter d_i (mm)	10	-
Reynolds number (-)	118–1479	88–3964

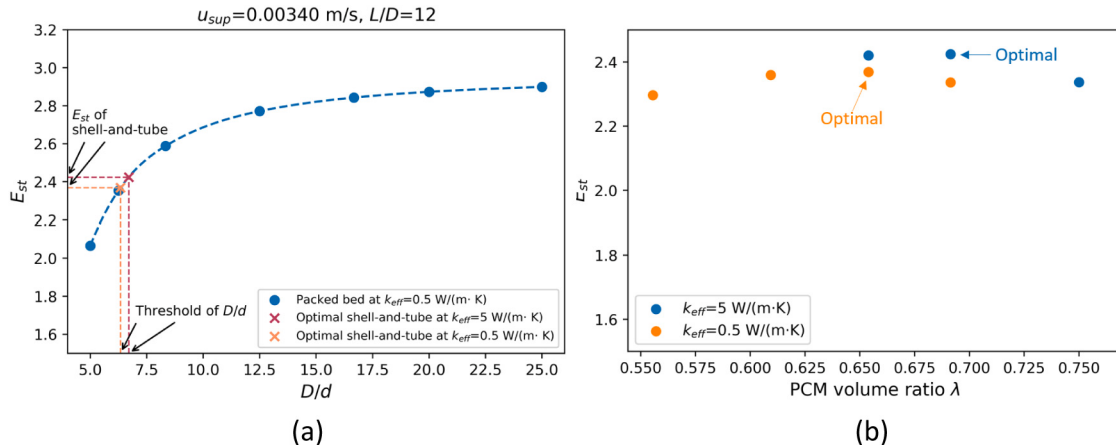


Fig. 9. The comparison of effective energy storage ratio, when $u_{\text{sup}} = 0.00340$ m/s, $L/D = 12$: (a) The threshold of D/d ; (b) Optimal PCM volume ratio for shell-and-tube

Fig. 10 summarizes the effective energy storage ratio E_{st} for shell-and-tube and packed bed units varying with the aspect ratio of the tank L/D under different superficial velocities. The dashed line exhibits

$E_{st} = 1$ for the sensible heat storage, which uses the same heat transfer fluid as the storage media and serves as the benchmark for the latent heat TES units. Shell-and-tube units show a higher E_{st} under a higher L/D

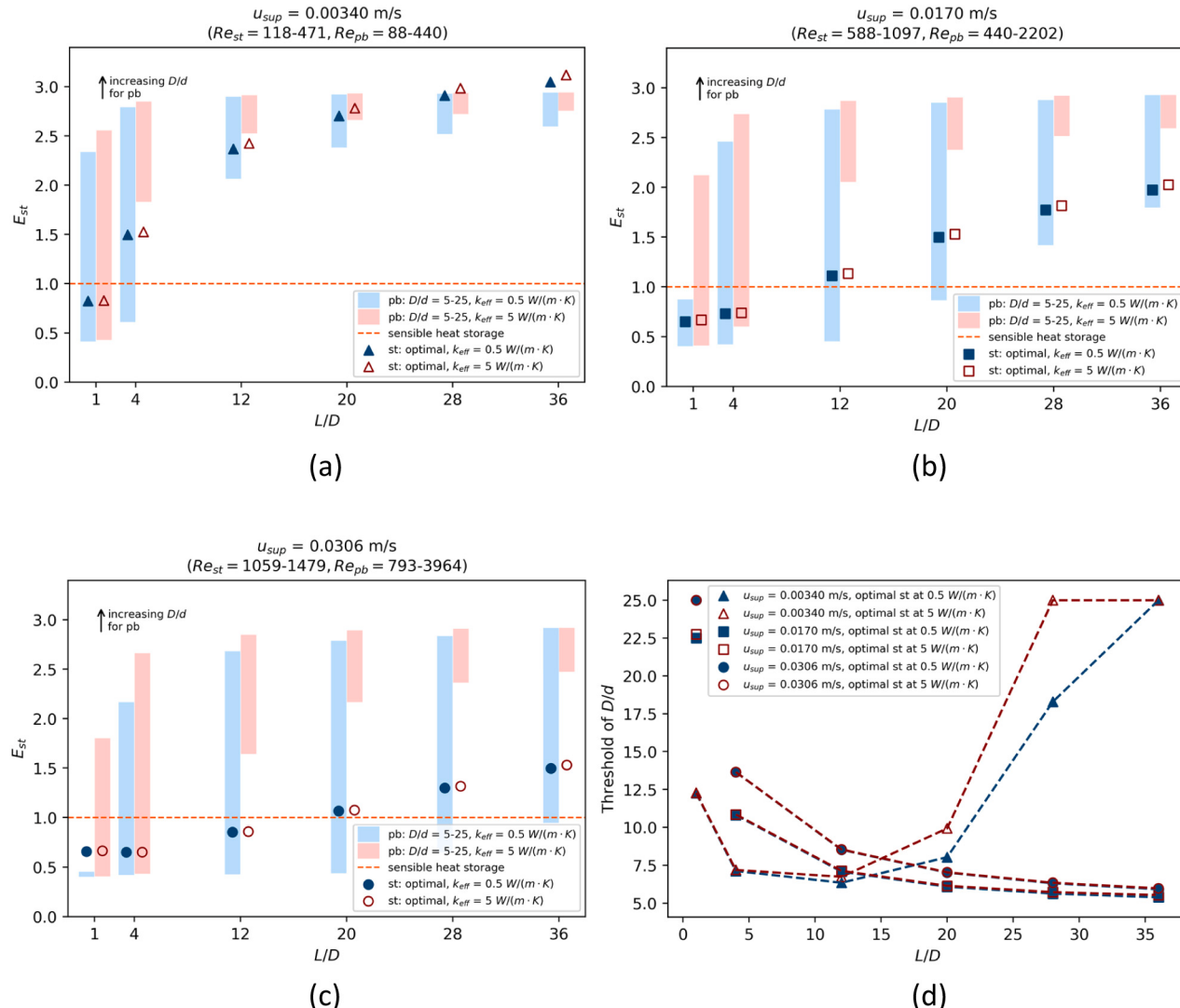


Fig. 10. The comparison of effective energy storage ratio E_{st} (pb: packed bed, st: shell-and-tube): (a) Superficial velocity: 0.00340 m/s; (b) Superficial velocity: 0.0170 m/s; (c) Superficial velocity: 0.0306 m/s; (d) Thresholds of D/d

or lower superficial velocity and it could be observed that the enhancement of E_{st} becomes more significant by increasing the effective thermal conductivity k_{eff} . For instance, when the superficial velocity is 0.00340 m/s, an enhanced k_{eff} of PCM from 0.5 to 5 W/(m · K) can increase E_{st} by 17.5% and 26.1%, respectively for a tank aspect ratio of 28 and 36. It is worth mentioning that when L/D is 36 in Fig. 10 (a), E_{st} of the shell-and-tube unit exceeds the maximal E_{st} of the packed bed unit. This is because the theoretical effective energy storage ratio $E_{st, \infty}$ in the packed bed is limited by the volume ratio of PCM capsules, which is around 0.6 for random close packing. In contrast, the PCM ratio could be more flexible in the shell-and-tube unit, and Fig. 10 (a) shows that by packing more than 80% PCM in the shell-and-tube tank, E_{st} could be over 3 after optimization. On the other hand, the packed bed unit shows its competitive storage performance under the high superficial velocity of HTF is mainly due to a higher surface-to-volume ratio, which contributes to a higher convective heat transfer coefficient. By increasing the diameter ratio D/d in the packed bed, the effective energy storage ratio E_{st} would increase towards the theoretical ratio $E_{st, \infty}$. Moreover, while shell-and-tube units could remain ineffective under a low tank aspect ratio ($L/D = 1, 4$), packed bed units exhibit the advantages of maintaining an effective energy storage ratio E_{st} higher than the benchmark. In this case, if the diameter ratio D/d is small enough in a packed bed, there is no significant necessity in enhancing the effective thermal conductivity in the shell-and-tube unit.

Fig. 10 (d) summarizes the thresholds of D/d of packed bed units from (a)-(c), compared with optimal shell-and-tube units with pure PCM, as shown in Fig. 9 (a) and Appendix A. When designing the packed bed unit, if the diameter ratio surpasses the threshold of D/d , it is reasonable to choose packed bed over shell-and-tube as the latent heat TES unit, as E_{st} is higher. A lower threshold of D/d means that it is easier for the packed bed to achieve the same storage performance as the shell-and-tube. As shown in Fig. 10 (d), the superficial velocity exhibits dominant influences on the threshold of D/d . When the superficial velocity is 0.0170 and 0.0306 m/s, the threshold of D/d is in the range of 5.3–13.6. It should be noticed that scatter points of 0.0170 and 0.0306 m/s when L/D is 1 are not connected with the line as both storage units are ineffective with $E_{st} < 1$. In comparison, the decrease of superficial velocity to 0.00340 m/s could greatly increase the threshold of D/d up to 25 under a higher tank aspect ratio of 36. Therefore, the shell-and-tube unit is more advantageous for low HTF superficial velocity scenarios with a large aspect ratio of tank L/D as a result of the optimization and enhancement of PCM thermal conductivity. The packed bed unit is more competitive under higher superficial velocities or lower tank aspect ratio, due to the effect of a large diameter ratio D/d on achieving a high E_{st} .

Figs. 11–12 respectively shows the PCM volume ratio, charging rate q_c and capacity effectiveness φ of the packed bed and shell-and-tube units. In Fig. 11, the range of PCM volume ratio remains around 0.6,

due to the assumption of random close packing. In contrast, the optimal PCM volume ratio in the shell-and-tube unit increases with increasing L/D and decreasing superficial velocity. Fig. 12 shows that the charging rate is mainly affected by the superficial velocity. For the shell-and-tube storage unit, the total charging rate for the tank can be estimated as the product of the charging rate for a single concentric cylinder unit and the number of tubes. The influences of superficial velocities could be explained by the fact that the enhancement of convection and thus a higher heat transfer rate occurs under higher superficial velocities. Overall, charging rates are on the same scale for shell-and-tube and packed bed units. As for the capacity effectiveness, in general, a larger L/D or smaller superficial velocity would lead to more complete charging for PCM for both shell-and-tube and packed bed units, as shown in Fig. 12. As the diameter ratio D/d is increasing to 25, the capacity effectiveness φ of the packed bed is approaching 1, which means nearly full exploitation of the storage potential using PCM.

3.4. Discussions

In summary, this study presents a quantitative demonstration of the threshold of choosing the packing bed unit, compared with the shell-and-tube design. As the packed bed storage unit has a larger heat transfer area between HTF and PCM, it can maintain a relatively high effective energy storage ratio E_{st} even when the HTF superficial velocity is large. For instance, better storage performance could be achieved by increasing the tank diameter D while keeping the capsule diameter d the same. For large-scale applications like concentrated solar power usually requiring large flow rates, the packed bed design is suitable as the threshold of D/d is at a low level, indicating that it is relatively easy for the packed bed to achieve the same energy storage performance as the shell-and-tube. In comparison, the storage performance of shell-and-tube could be significantly enhanced by optimization and using PCM composite with higher effective thermal conductivities k_{eff} . Hence, shell-and-tube storage units are more suitable for small-scale applications like domestic solar water heating. With long tubes inside the shell-and-tube unit, the effective energy storage ratio E_{st} could be increased significantly due to the flexibility of changing the PCM volume ratio and the effective thermal conductivity of PCM.

It should be noted that the variation of the diameter ratio for parametric studies in the packed bed unit is achieved mainly by changing the capsule diameter d . The values of the thresholds of D/d may vary depending on other parameters. For example, the tank diameter D for both units and the inner tube diameter d_i in shell-and-tube units are fixed in this work, but may exert influences on the thresholds of D/d . In the future, their impacts could be examined, and the concept and methodology developed in this work can be generalized to other applications using different PCM types to design packed bed storage units.

The purpose of this study is to illustrate a framework to compare the

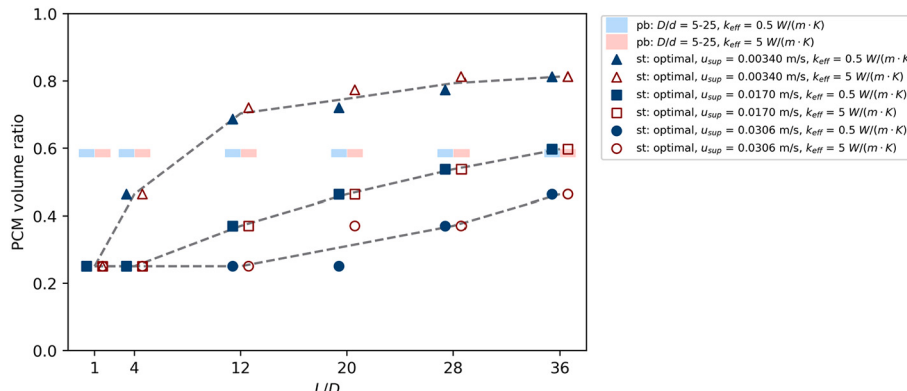


Fig. 11. The comparison of PCM volume ratio (pb: packed bed, st: shell-and-tube)

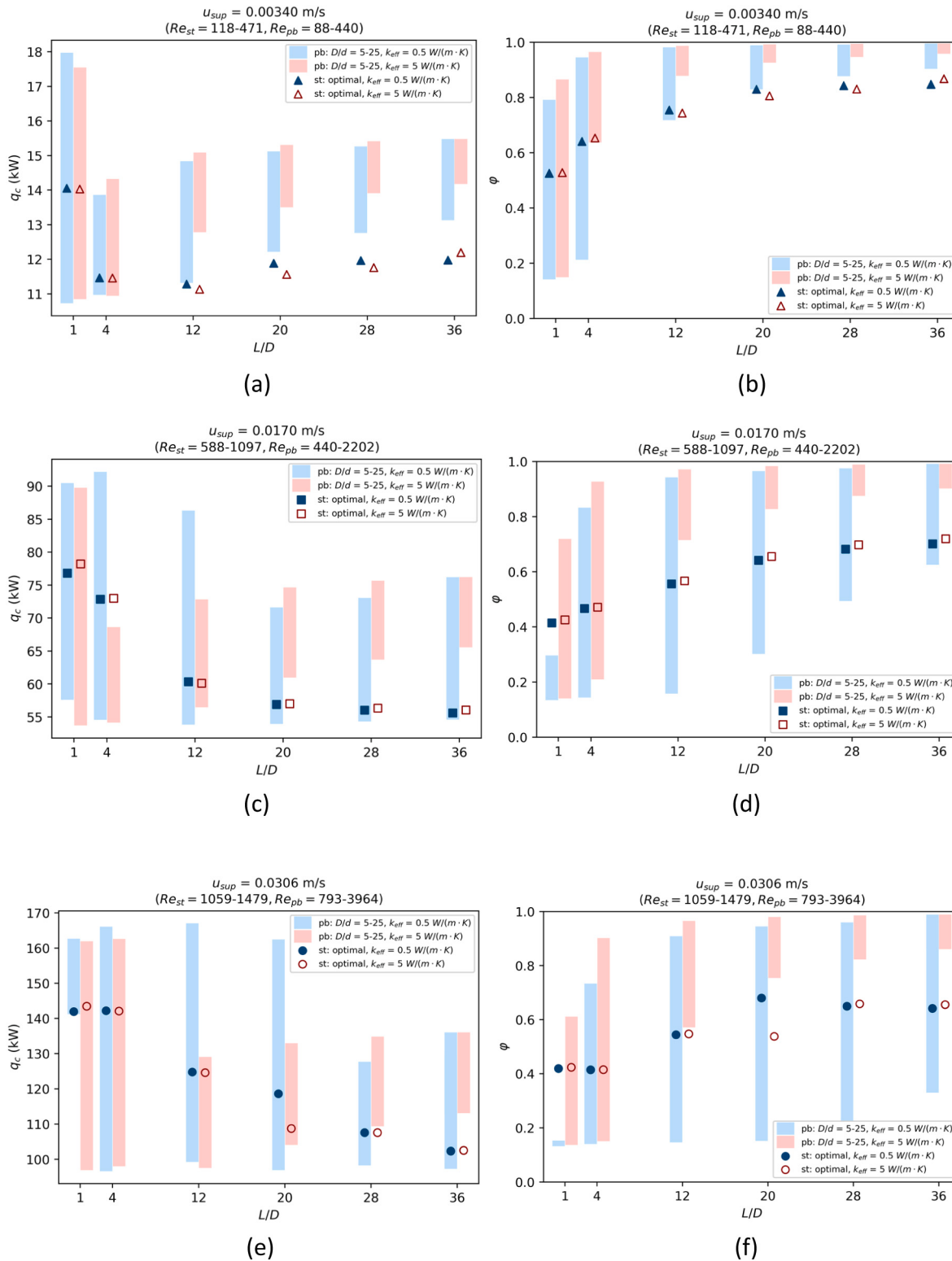


Fig. 12. The comparison of charging rate q_c and capacity effectiveness φ (pb: packed bed, st: shell-and-tube): (a) Charging rate q_c with a superficial velocity of 0.00340 m/s; (b) Capacity effectiveness φ with a superficial velocity of 0.00340 m/s; (c) Charging rate q_c with a superficial velocity of 0.0170 m/s; (d) Capacity effectiveness φ with a superficial velocity of 0.0170 m/s; (e) Charging rate q_c with a superficial velocity of 0.0306 m/s; (f) Capacity effectiveness φ with a superficial velocity of 0.0306 m/s.

storage performance of the shell-and-tube and packed bed LHTES units. The geometric parameters of TES unit design and properties of fluid and PCM are the main concerns in this study. For future investigation regarding the impacts of other parameters on the energy storage

performance comparison, the proposed framework could be adopted and applied for analysis. For example, when investigating the material aspects for capsules and tubes, the tube in the shell-and-tube design could be considered by adding a thin layer at the interface between fluid

and PCM, while the influences of shell materials on the heat transfer in the packed bed design can be reflected by incorporating the thermal properties of shell into the effective thermal properties (via updating the conductivity and capacity through e.g., effective media theory) of the packed bed units. As for the discharging process with solidifying PCM, there could appear more than one solidification point and the effective specific heat method used in this framework could consider the multi peaks showed up in the DSC thermograph, by implementing directly the experimental data for describing the phase change behavior.

4. Conclusions

In this paper, a comprehensive numerical study on the performance evaluation of the packed bed LHTES unit and comparison with the shell-and-tube storage unit is carried out. The influences of geometric parameters and effective thermal conductivity in packed bed systems were investigated. The threshold of D/d was defined when the packed bed unit shows the same effective energy storage ratio E_{st} as one of the shell-and-tube units. Two scenarios of the shell-and-tube unit were studied as the benchmark for comparison: (1) under optimal PCM volume ratio when using pure PCM with effective thermal conductivity of $0.5 \text{ W}/(\text{m} \cdot \text{K})$; (2) under optimal PCM volume ratio when using PCM with enhanced effective thermal conductivity $5 \text{ W}/(\text{m} \cdot \text{K})$. The comparison has been analyzed under different superficial velocities and aspect ratios of the tank. The thresholds D/d for the packed bed are found, above which the effective energy storage capacity of the packed bed would be higher than that of an optimal shell-and-tube unit. The threshold D/d can be quantitatively correlated to the HTF superficial velocity, providing a pathway for the tailored design of thermal storage systems.

- When designing the packed bed TES units using PCM, smaller capsules, longer tanks and larger tank diameters would be preferred for purpose of maximizing the effective energy storage ratio E_{st} . The dimensionless scaling shows that when either the diameter ratio D/d is larger than 8 or the length ratio L/d is larger than 45, the packed bed LHTES system could be ensured to be effective, i.e. $E_{st} > 1$.
- In the packed bed storage unit, a higher effective thermal conductivity k_{eff} would increase the effective energy storage ratio and the enhancement effect is significant when the diameter ratio D/d is smaller than 15. This is because the convection effect is weak under a low diameter ratio and thus the decrease of PCM thermal resistance by increasing k_{eff} contributes more to the enhancement of effective energy storage ratio.
- The value of the threshold of D/d informs the designer whether to choose the packed bed or the shell-and-tube storage unit. A smaller

threshold of D/d indicates that it is easier for the packed bed unit to reach the same effective energy storage performance as the shell-and-tube unit. The threshold of D/d is up to 25 under a lower HTF superficial velocity (0.00340 m/s), while is $5.3\text{--}13.6$ under a higher HTF superficial velocity ($0.0170, 0.0306 \text{ m/s}$).

- When the superficial velocity is 0.00340 m/s , an enhanced k_{eff} of PCM from 0.5 to $5 \text{ W}/(\text{m} \cdot \text{K})$ can increase E_{st} by 17.5% and 26.1% , respectively for a tank aspect ratio L/D of 28 and 36 . In this case, the effective energy storage ratio of shell-and-tube units could surpass the theoretical effective energy storage ratio in the packed bed.
- When the HTF superficial velocity is large, the packed bed storage unit can maintain a large surface-to-volume ratio by increasing the diameter ratio D/d and therefore can reach a high effective energy storage ratio E_{st} . In comparison, when the superficial velocity is low, the storage performance of shell-and-tube could be remarkably enhanced by optimization and using PCM composite with higher effective thermal conductivities k_{eff} .

Through comparative analysis it was found that the packed bed PCM unit is more suitable to be applied under higher flow rates and thus more advantageous for large-scale applications like concentrated solar power plants, while shell-and-tube storage units are more suitable for small-scale applications like domestic solar water heating. The performance evaluation and comparison framework based on the numerical analysis presented in this paper can serve as a guideline to design packed bed thermal energy storage systems using PCM in comparison with traditional shell-and-tube units under specific geometric and operational conditions.

CRediT authorship contribution statement

Haobin Liang: Conceptualization, Methodology, Validation, Investigation, Writing – original draft, Visualization. **Jianlei Niu:** Methodology, Writing – review & editing, Supervision. **Ratna Kumar Annabattula:** Methodology, Writing – review & editing. **K.S. Reddy:** Methodology, Writing – review & editing. **Ali Abbas:** Writing – review & editing. **Minh Tri Luu:** Writing – review & editing. **Yixiang Gan:** Conceptualization, Methodology, Writing – review & editing, Supervision.

Declaration of competing interest

The authors declare that they have no known competing financial interests or personal relationships that could have appeared to influence the work reported in this paper.

Appendix A. The effect of geometric parameters on the packed bed

A.1. Capsule diameter d

The tank diameter and tank height were fixed at 0.25 m and 2 m , respectively, to investigate the influence of capsule diameter d on the effective energy storage ratio E_{st} . Seven different capsule diameters were chosen from 10 mm to 50 mm . The void fraction ε varies from 0.403 to 0.426 . The effects of d on T_{out} and E_{st} are shown in Fig. A1.

The capsule diameter d is crucial to the heat transfer process and energy storage performance of the packed bed system. It directly affects the void fraction ε and more importantly, the heat transfer coefficient h_{eff} , according to Eqs. (16)–(19). As shown in Fig. A1 (a), with decreasing capsule diameter, and it generally takes a longer time to reach the specified heat transfer effectiveness of 80% . The slower outlet temperature increase of smaller capsules indicates that the heat transfer rate between HTF and PCM is higher. This is mainly because lower d leads to larger heat transfer area between two domains, which is reflected in larger h_{inter} in the governing equations. Therefore, as shown in Fig. A1 (b), E_{st} is higher when the capsule diameter d is smaller. Moreover, as d decreases, the theoretical energy storage ratio $E_{st,\infty}$ increases. This is due to the drop of void fraction ε when decreasing d , which means that the packing ratio of PCM is higher. The faster increase in E_{st} than $E_{st,\infty}$ proves the effectiveness of decreasing diameter in enhancing the effective energy storage performance of packed bed TES systems.

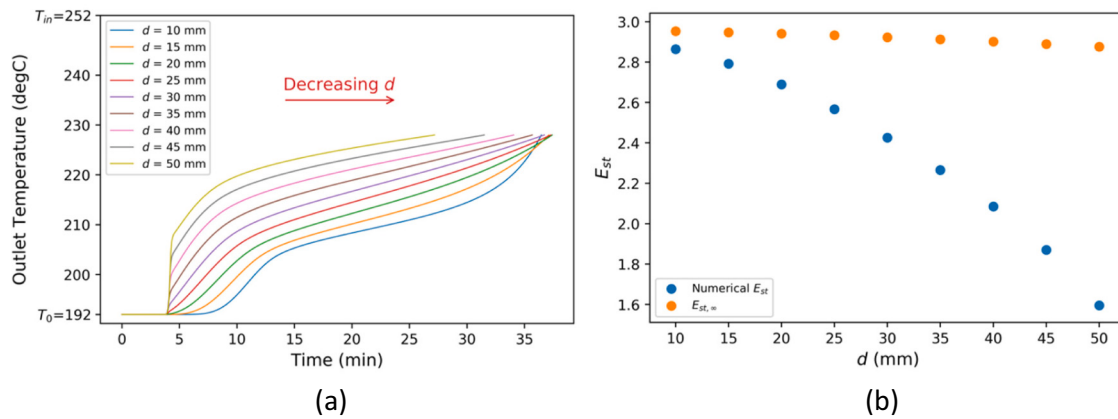


Fig. A1. With fixed $D = 0.25$ m, $L = 2$ m: (a) The effect of capsule diameter d on T_{out} ; (b) The effect of capsule diameter d on E_{st} .

A.2. Tank diameter D

When investigating the influences of tank diameter D on the effective storage performance, the capsule diameter and tank height were set as 30 mm and 2 m. The tank diameter D varies from 0.15 m to 0.75 m, with an interval of 0.1 m. Therefore, the corresponding void fraction ε is in the range of 0.412–0.426. The impact of D on HTF outlet temperature T_{out} and effective energy storage ratio E_{st} are shown in Fig. A2.

The influence of tank diameter is reflected in the tank void fraction, according to Eq. (21). With the increase of D , the void fraction ε drops. Hence, the theoretical energy storage capacity Q_∞ due to larger amount packing of PCM, resulting in a higher $E_{st,\infty}$. Besides, the reduction of ε leads to a higher particle surface area per unit volume a_p , which increases the heat transfer coefficient h_{eff} between HTF and PCM. Therefore, the enhancement of E_{st} with increasing D could be observed from Fig. A2 (b). Besides, as shown in Fig. A2 (a), stronger heat transfer between HTF and PCM leads to a longer time for the outlet temperature to reach the specified one.

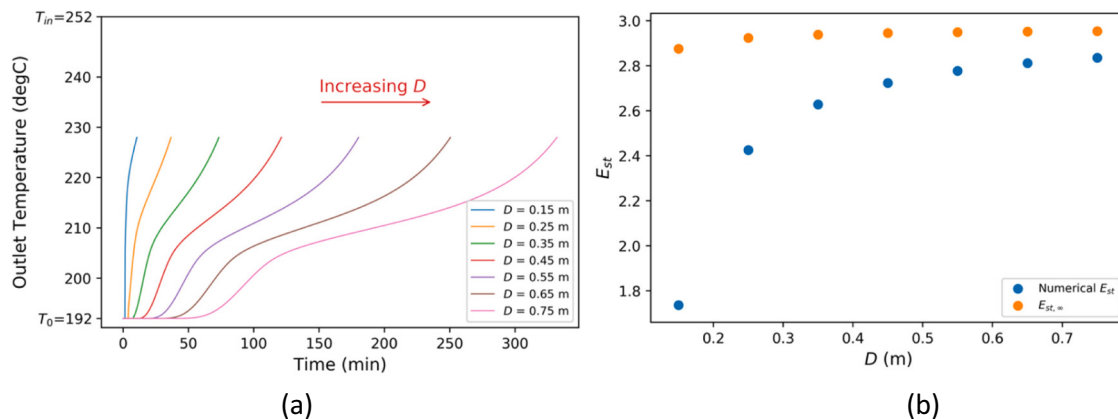


Fig. A2. With fixed $d = 30$ mm, $L = 2$ m: (a) The effect of tank diameter D on T_{out} ; (b) The effect of tank diameter D on E_{st} .

On the other hand, the decrease of void fraction while increasing tank diameter would also lead to a higher pressure drop, according to Eq. (29). However, similar to the calculation of pressure drop for varying capsule diameter in section A1, the energy consumption could be neglected considering the thermal energy stored in the system. The energy ratios Q_{pump}/Q_{eff} for all cases are lower than 1e-5%.

A.3. Tank height L

Finally, the influence of the tank height L was investigated through parametric studies: Ten sets of numerical simulation with L varying from 0.5 m to 4 m. The tank diameter and capsule diameter were kept the same, i.e. 0.25 m and 30 mm, respectively. The impacts of L on HTF outlet temperature T_{out} and effective energy storage ratio E_{st} are shown in Fig. A3.

As D and d are fixed, the void fraction and heat transfer coefficient does not change throughout the parametric studies. Thus, the theoretical energy storage ratios $E_{st,\infty}$ are the same for different tank heights, shown in Fig. A3 (b). The increase of the effective energy storage time and the increase of the effective energy storage ratio E_{st} are due to a higher effective heat transfer length between HTF and PCM as tank length L increases. It should be noted that under specified conditions, the packed bed storage unit shows ineffective energy storage when the tank height is small as 0.5 m. This means that when designing a packed bed LHTES unit, the tank height should be ensured to be larger than the minimal length, which is 1 m in this study. Otherwise, a packed bed unit with sensible heat storage should be considered. The increase of pressure drop was investigated and the results show that the energy ratio Q_{pump}/Q_{eff} is lower than 1e-6% even when L is 4 m, which means that the energy consumption can be neglected when considering the tank height.

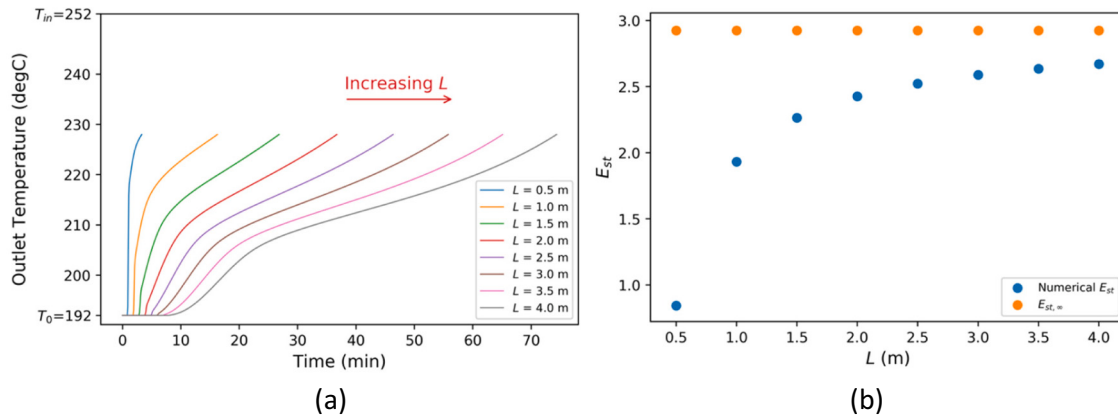


Fig. A3. With fixed $D = 0.25$ m, $d = 30$ mm: (a) The effect of tank height L on T_{out} ; (b) The effect of tank height L on E_{st} .

Appendix B. Shell-and-tube and packed bed unit comparison under different superficial velocity and tank height

This section exhibits the unit performance comparison under different superficial velocities and tank heights. The capsule diameters d of 10, 12.5, 15, 20, 30, 40 and 40 mm were applied for the packed bed unit, and the diameter ratios D/d varied between 5 and 25. Meanwhile, the flow is laminar in the shell-and-tube system. The following scenarios have been considered: (1) low superficial velocity of 0.00340 m/s in Fig. B1; (2) medium superficial velocity of 0.0170 m/s in Fig. B2; and (3) high superficial velocity of 0.0306 m/s in Fig. B3.

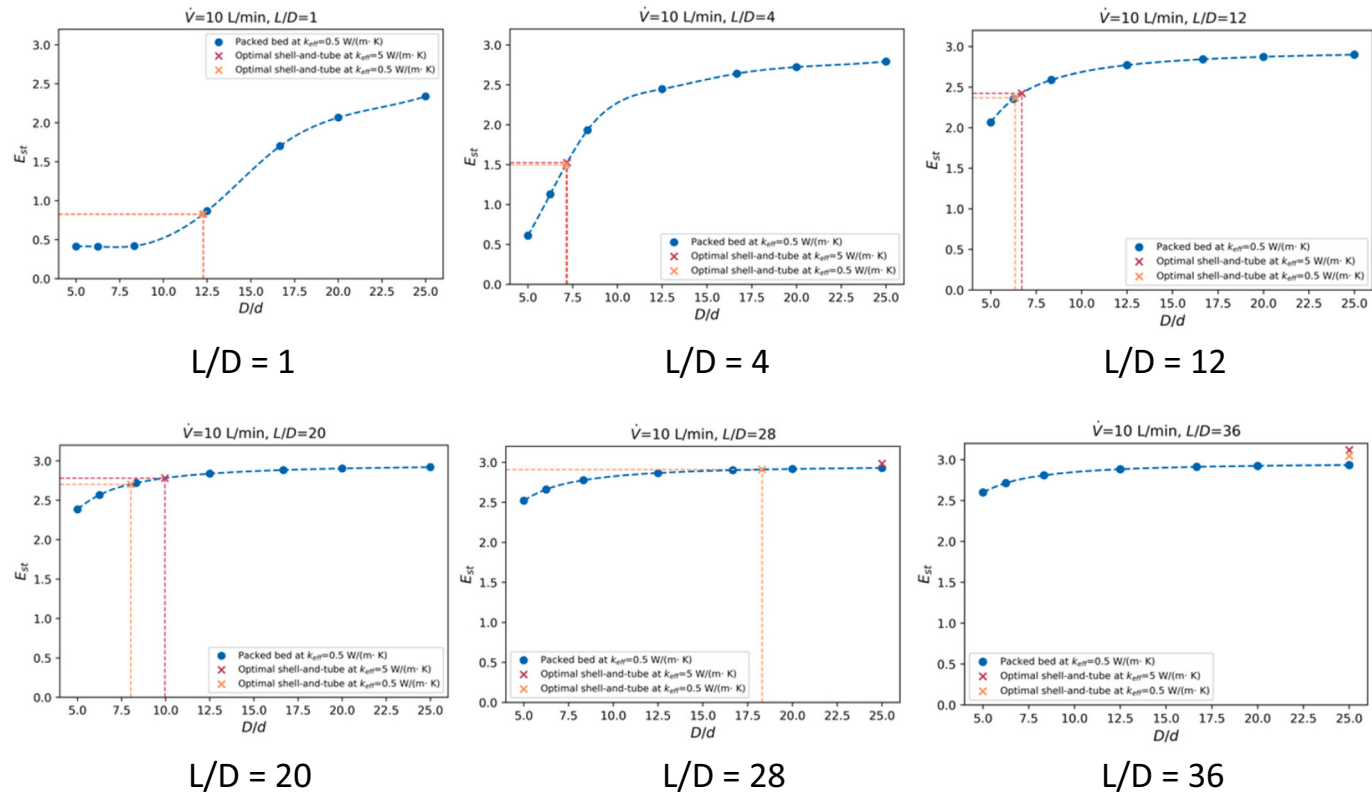


Fig. B1. Superficial velocity: 0.00340 m/s (flow rate: 10 l/min)

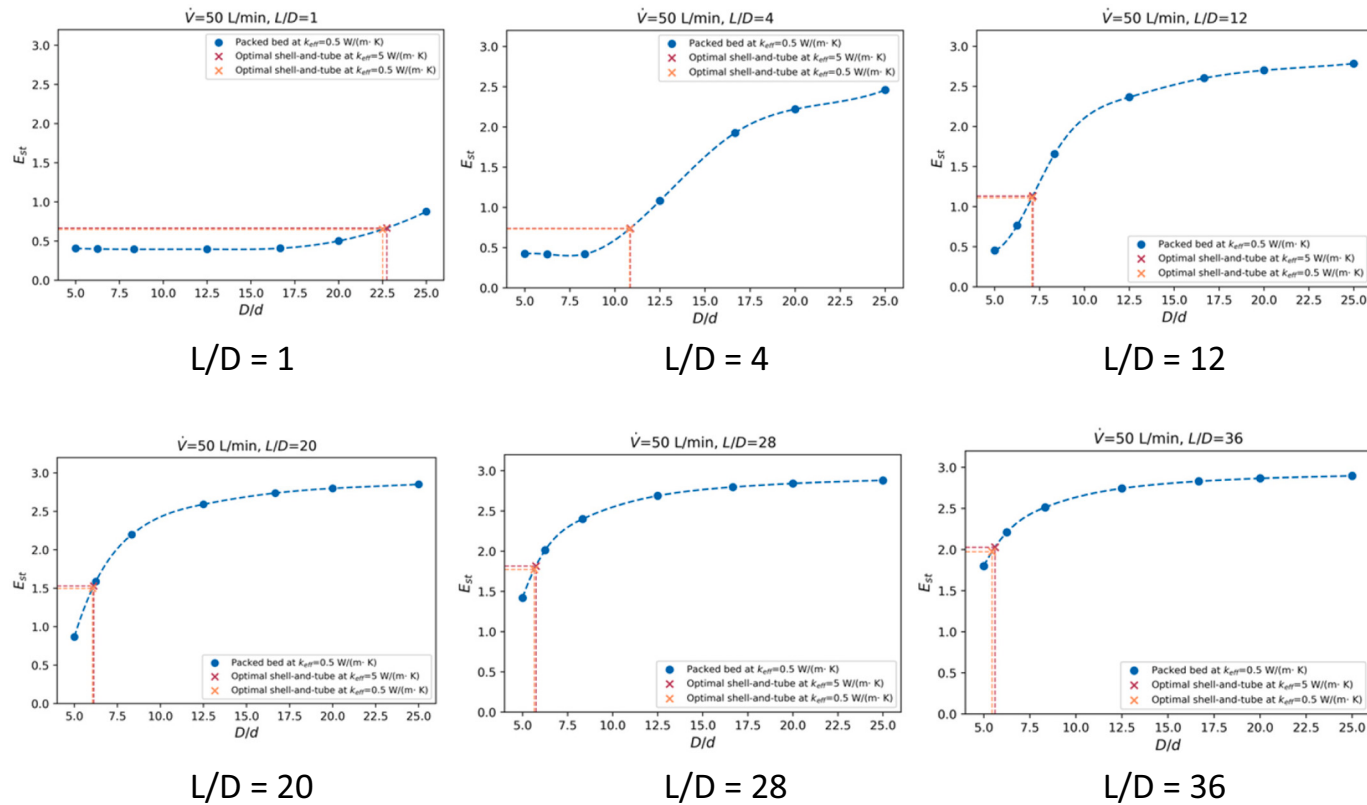


Fig. B2. Superficial velocity: 0.0170 m/s (flow rate: 50 l/min)

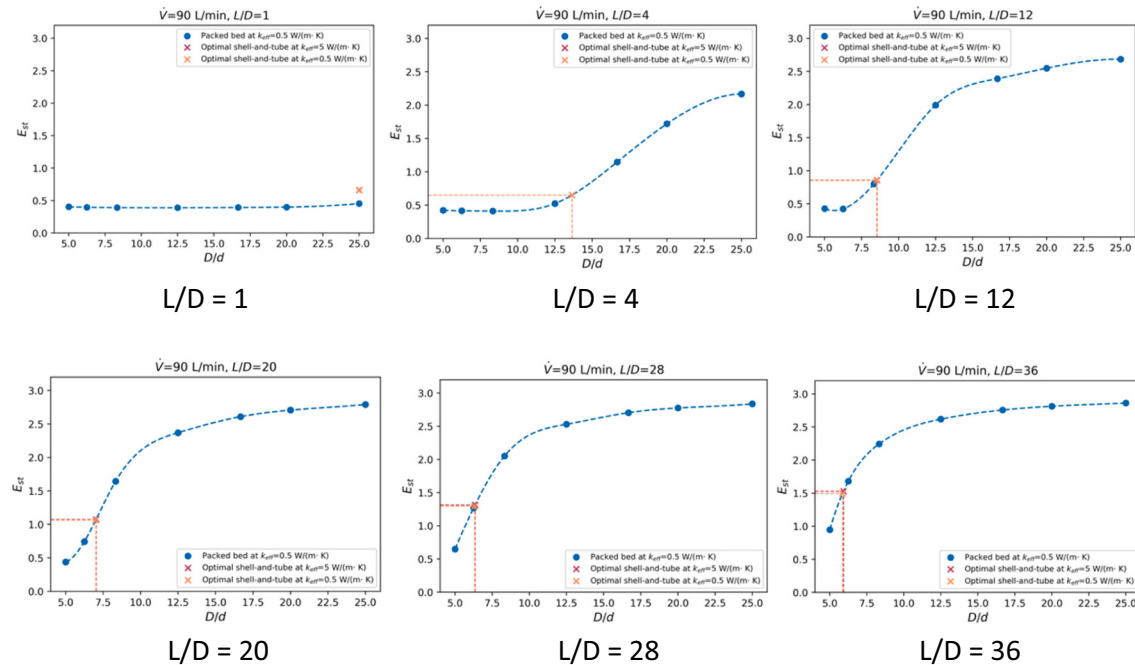


Fig. B3. Superficial velocity: 0.0306 m/s (flow rate: 90 l/min)

References

- [1] BP Energy Outlook 2019, BP Energy, 2019.
- [2] Renewable Power Generation Costs in 2018, International Renewable Energy Agency (IRENA), 2019.
- [3] H. Nazir, et al., Recent developments in phase change materials for energy storage applications: a review, Int. J. Heat Mass Transf. 129 (2019) 491–523.
- [4] H. Liang, et al., Towards idealized thermal stratification in a novel phase change emulsion storage tank, Appl. Energy 310 (2022), 118526.

- [5] L. Liu, et al., Cooling storage performance of a novel phase change material nano-emulsion for room air-conditioning in a self-designed pilot thermal storage unit, *Appl. Energy* 308 (2022), 118405.
- [6] B. Zalba, et al., Review on thermal energy storage with phase change: materials, heat transfer analysis and applications, *Appl. Therm. Eng.* 23 (3) (2003) 251–283.
- [7] Z. Khan, Z. Khan, A. Ghafoor, A review of performance enhancement of PCM based latent heat storage system within the context of materials, thermal stability and compatibility, *Energy Convers. Manag.* 115 (2016) 132–158.
- [8] V. Mayilvelathan, Arasu A. Valan, Experimental investigation on thermal behavior of graphene dispersed erythritol PCM in a shell and helical tube latent energy storage system, *Int. J. Therm. Sci.* 155 (2020), 106446.
- [9] T. Nomura, et al., High thermal conductivity phase change composite with percolating carbon fiber network, *Appl. Energy* 154 (2015) 678–685.
- [10] Y. Tian, C.Y. Zhao, A numerical investigation of heat transfer in phase change materials (PCMs) embedded in porous metals, *Energy* 36 (9) (2011) 5539–5546.
- [11] R. Velraj, et al., Heat transfer enhancement in a latent heat storage system, *Sol. Energy* 65 (3) (1999) 171–180.
- [12] M.J. Hosseini, M. Rahimi, R. Bahrampoury, Experimental and computational evolution of a shell and tube heat exchanger as a PCM thermal storage system, *Int. Commun. Heat Mass Transf.* 50 (2014) 128–136.
- [13] Y. Dutil, et al., A review on phase-change materials: mathematical modeling and simulations, *Renew. Sust. Energ. Rev.* 15 (1) (2011) 112–130.
- [14] K.S. Reddy, V. Mudgal, T.K. Mallick, Review of latent heat thermal energy storage for improved material stability and effective load management, *J. Energy Storage* 15 (2018) 205–227.
- [15] N. Nallusamy, S. Sampath, R. Velraj, Experimental investigation on a combined sensible and latent heat storage system integrated with constant/varying (solar) heat sources, *Renew. Energ.* 32 (7) (2007) 1206–1227.
- [16] S. Wu, G. Fang, Dynamic performances of solar heat storage system with packed bed using myristic acid as phase change material, *Energy Build.* 43 (5) (2011) 1091–1096.
- [17] Regin A. Felix, S.C. Solanki, J.S. Saini, An analysis of a packed bed latent heat thermal energy storage system using PCM capsules: numerical investigation, *Renew. Energ.* 34 (7) (2009) 1765–1773.
- [18] R. Al-Shanaq, B. Young, M. Farid, Cold energy storage in a packed bed of novel graphite/PCM composite spheres, *Energy* 171 (2019) 296–305.
- [19] X. Jia, X. Zhai, X. Cheng, Thermal performance analysis and optimization of a spherical PCM capsule with pin-fins for cold storage, *Appl. Therm. Eng.* 148 (2019) 929–938.
- [20] L.-W. Fan, et al., An experimental and numerical investigation of constrained melting heat transfer of a phase change material in a circumferentially finned spherical capsule for thermal energy storage, *Appl. Therm. Eng.* 100 (2016) 1063–1075.
- [21] H.B. Liu, C.Y. Zhao, Effect of radial porosity oscillation on the thermal performance of packed bed latent heat storage, *Engineering* 7 (4) (2021) 515–525.
- [22] A. Kumar, S.K. Saha, Thermal and structural characterizations of packed bed thermal energy storage with cylindrical micro-encapsulated phase change materials, *J. Energy Storage* 48 (2022), 103948.
- [23] M. Grabo, E. Acar, E.Y. Kenig, Modeling and improvement of a packed bed latent heat storage filled with non-spherical encapsulated PCM-elements, *Renew. Energ.* 173 (2021) 1087–1097.
- [24] A. Abdulla, K.S. Reddy, Comparative study of single and multi-layered packed-bed thermal energy storage systems for CSP plants, *Appl. Sol. Energy* 53 (3) (2017) 276–286.
- [25] E. Alptekin, M.A. Ezan, A systematic assessment on a solar collector integrated packed-bed single/multi-layered latent heat thermal energy storage system, *J. Energy Storage* 37 (2021), 102410.
- [26] A. Mawire, C.S. Ekwomadu, A.B. Shobo, Experimental charging characteristics of medium-temperature cascaded packed bed latent heat storage systems, *J. Energy Storage* 42 (2021), 103067.
- [27] K. Nagano, et al., Thermal characteristics of a direct heat exchange system between granules with phase change material and air, *Appl. Therm. Eng.* 24 (14) (2004) 2131–2144.
- [28] M. Wu, C. Xu, Y.-L. He, Dynamic thermal performance analysis of a molten-salt packed-bed thermal energy storage system using PCM capsules, *Appl. Energy* 121 (2014) 184–195.
- [29] M.-J. Li, et al., Experimental and numerical study on the performance of a new high-temperature packed-bed thermal energy storage system with macroencapsulation of molten salt phase change material, *Appl. Energy* 221 (2018) 1–15.
- [30] M. Cheralathan, R. Velraj, S. Renganarayanan, Heat transfer and parametric studies of an encapsulated phase change material based cool thermal energy storage system, *J. Zhejiang Univ. Sci. A* 7 (11) (2006) 1886–1895.
- [31] S. Wu, G. Fang, X. Liu, Thermal performance simulations of a packed bed cool thermal energy storage system using n-tetradecane as phase change material, *Int. J. Therm. Sci.* 49 (9) (2010) 1752–1762.
- [32] K.A.R. Ismail, R. Stuginsky Jr., A parametric study on possible fixed bed models for pcm and sensible heat storage, *Appl. Therm. Eng.* 19 (7) (1999) 757–788.
- [33] S. Karthikeyan, R. Velraj, Numerical investigation of packed bed storage unit filled with PCM encapsulated spherical containers – a comparison between various mathematical models, *Int. J. Therm. Sci.* 60 (2012) 153–160.
- [34] A. de Gracia, L.F. Cabeza, Numerical simulation of a PCM packed bed system: a review, *Renew. Sust. Energ. Rev.* 69 (2017) 1055–1063.
- [35] F. Agyenim, et al., A review of materials, heat transfer and phase change problem formulation for latent heat thermal energy storage systems (LHTESS), *Renew. Sust. Energ. Rev.* 14 (2) (2010) 615–628.
- [36] H. Liang, J. Niu, Y. Gan, Performance optimization for shell-and-tube PCM thermal energy storage, *J. Energy Storage* 30 (2020), 101421.
- [37] Y. Fang, J. Niu, S. Deng, Numerical analysis for maximizing effective energy storage capacity of thermal energy storage systems by enhancing heat transfer in PCM, *Energy Build.* 160 (2018) 10–18.
- [38] K. Nithyanandam, R. Pitchumani, A. Mathur, Analysis of a latent thermocline storage system with encapsulated phase change materials for concentrating solar power, *Appl. Energy* 113 (2014) 1446–1460.
- [39] M. Belusko, E. Halawa, F. Bruno, Characterising PCM thermal storage systems using the effectiveness-NTU approach, *Int. J. Heat Mass Transf.* 55 (13) (2012) 3359–3365.
- [40] Y. Fang, J. Niu, S. Deng, An analytical technique for the optimal designs of tube-in-tank thermal energy storage systems using PCM, *Int. J. Heat Mass Transf.* 128 (2019) 849–859.
- [41] F.P. Incropera, et al., *Fundamentals of Heat and Mass Transfer*, Wiley, 2007.
- [42] T. Esence, et al., A review on experience feedback and numerical modeling of packed-bed thermal energy storage systems, *Sol. Energy* 153 (2017) 628–654.
- [43] B. Xu, P.-W. Li, C.L. Chan, Extending the validity of lumped capacitance method for large biot number in thermal storage application, *Sol. Energy* 86 (6) (2012) 1709–1724.
- [44] H. Shamsi, M. Boroushaki, H. Geraei, Performance evaluation and optimization of encapsulated cascade PCM thermal storage, *J. Energy Storage* 11 (2017) 64–75.
- [45] N. Wakao, S. Kaguei, T. Funazkri, Effect of fluid dispersion coefficients on particle-to-fluid heat transfer coefficients in packed beds: correlation of Nusselt numbers, *Chem. Eng. Sci.* 34 (3) (1979) 325–336.
- [46] A.G. Dixon, Correlations for wall and particle shape effects on fixed bed bulk voidage, *Can. J. Chem. Eng.* 66 (5) (1988) 705–708.
- [47] A.G. Dixon, Heat transfer in fixed beds at very low (<4) tube-to-particle diameter ratio, *Ind. Eng. Chem. Res.* 36 (8) (1997) 3053–3064.
- [48] Q. Xie, Q. Zhu, Y. Li, Thermal storage properties of molten nitrate salt-based nanofluids with graphene nanoplatelets, *Nanoscale Res. Lett.* 11 (1) (2016) 306.
- [49] https://www.therminol.com/sites/therminol/files/documents/TF09A_Therminol_VP1.pdf.
- [50] W. Dai, D. Hanaor, Y. Gan, The effects of packing structure on the effective thermal conductivity of granular media: a grain scale investigation, *Int. J. Therm. Sci.* 142 (2019) 266–279.